The use of zirconia-based solid electrolytes for the rapid determination of iron oxide activities in iron- and steel-making slags

by M.J.U.T. VAN WIJNGAARDEN* and R.J. DIPPENAAR†

SYNOPSIS

An electrochemical technique based on the solid oxide galvanic cell

$$Mo / Mo + MoO_2 / ZrO_2\text{-}MgO / Fe + (Fe_xO)_{slag} + Ag / Fe$$

was used in a determination of Fe_xO activities in liquid slag systems. The emf measurements, scanning electron microscopy, and microprobe analysis of the cross-sections of the electrolyte tubes used in direct contact with the slag melts indicated that slag attack did not affect the open-circuit emf values during normal cell operation. The reliability of the cell was confirmed by the good agreement between the standard free energy of formation of liquid Fe_xO obtained in the present study and those reported in the literature. The Fe_xO activities were determined in $Fe_xO\text{-}CaO$ and $Fe_xO\text{-}SiO_2$ slags at 1673 K, and are in good agreement with those measured by the conventional gas-equilibrium technique. The experimental technique was successfully extended to the measurement of Fe_xO activities in the complex slags that are used for the external desiliconization of the hot metal product of the blast furnace.

SAMEVATTING

'n Elektrochemiese tegniek, gebaseer op die vaste-oksied galvaniese sel

$$Mo / Mo + MoO_2 / ZrO_2\text{-}MgO / Fe + (Fe_xO)_{slak} + Ag / Fe$$

is gebruik vir die bepaling van Fe_xO aktiwiteite in gesmelte slaksisteme. Emf metings, aftas elektronmikroskopie en mikrosonde analises van die dwarsdeursnee van die elektroliet buisies wat in direkte kontak met die slak gebruik is, het getoon dat slakaanval nie die oop-baan emf tydens normale metings beïnvloed nie. Die betroubaarheid van die sel is bevestig deur die goeie korrelasie wat verkry is tussen die eksperimenteel bepaalde standaardvrye vormingsenergie van gesmelte Fe_xO, en waardes wat in die literatuur gerapporteer is. Fe_xO aktiwiteite is bepaal in $Fe_xO\text{-}CaO$ en $Fe_xO\text{-}SiO_2$ slakke by 1673 K en stem goed ooreen met aktiwiteite wat met konvensionele gas-ewewigtegnieke gemeet is. Die eksperimentele tegniek is suksesvol deurgevoer vir die bepaling van Fe_xO aktiwiteite in komplekse slakke wat gebruik word vir die eksterne desilikonisering van ru-yster afkomstig uit die hoogoond.

Introduction

In recent years there has been a constant search for effective and economic refining processes for the removal of sulphur and phosphorus from the hot-metal product of the blast furnace. The Japanese steel industry, in particular, has made a major contribution towards the research and development of these processes[1,2]. However, Japanese iron- and steelmakers are primarily concerned with the removal of phosphorus from the blast-furnace hot metal, and have concentrated most of their efforts on the optimization of phosphorus removal[3]. South African blast furnaces, on the other hand, produce hot metal with a relatively high sulphur content, which has resulted in a strong tendency by the local steel industry to develop external refining processes for the simultaneous removal of sulphur and phosphorus. However, this simultaneous removal is impeded by the divergent conditions necessary for effective desulphurization and

dephosphorization. For example, effective dephosphorization is enhanced by high iron oxide activity in the slag; in contrast, sulphur removal is favoured by low iron oxide activity. The key to better control of sulphur and phosphorus levels in the hot metal is, therefore, a detailed knowledge of iron oxide activity in slag. There is therefore a need for the rapid determination of iron oxide activities in slag systems typical of those used in the South African steel industry. This need led to the development of an experimental technique that can be used for the rapid and quantitative assessment of iron oxide activity in liquid slag systems.

Very few attempts were made in the past to measure the iron oxide activity of slags directly because it was found that the solid electrolytes used dissolved very rapidly in the slags of interest in iron- and steel-making processes. However, Iwase *et al.*[4] recently demonstrated that the problems with slag attack can be overcome, and that the iron oxide activities in liquid slags can indeed be directly assessed. They used solid electrolytes of magnesia-stabilized zirconia in a cell arrangement that permitted the effective and rapid direct measurement of iron oxide activities in metallurgical slags. The principles

* Lecturer.
† Professor.
  Both the above of the Department of Materials Science and Metallurgical Engineering, University of Pretoria, Hatfield, Pretoria 0083.
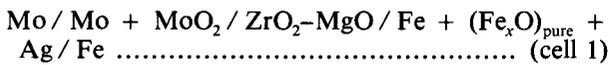
laid down by Iwase *et al.* were adhered to in the development of the experimental technique used in the present investigation.
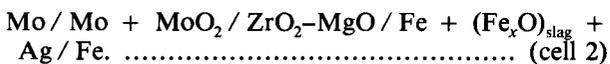
This paper reports on the experimental conditions pertaining to this new experimental technique and on the way it is applied. The influence of slag attack on the measured iron oxide activities is discussed, and the reliability and accuracy of the measured values are evaluated. Iron oxide activities, determined in synthetic and in complex industrial slags, are reported and discussed.

Theoretical Aspects

Pure liquid iron oxide in contact with iron is non-stoichiometric, and the chemical formula is usually expressed as Fe_xO ($x < 1$). The measurement of Fe_xO activity can be achieved most directly by use of the following two galvanic cells:

$$Mo / Mo + MoO_2 / ZrO_2-MgO / Fe + (Fe_xO)_{pure} + Ag / Fe \dots \dots \dots \dots (cell \; 1)$$

and

$$Mo / Mo + MoO_2 / ZrO_2-MgO / Fe + (Fe_xO)_{slag} + Ag / Fe. \dots \dots \dots \dots (cell \; 2)$$

A combination of the emf's of cells 1 and 2 gives the emf of the cell:

$$Fe / Fe + (Fe_xO)_{pure} + Ag / ZrO_2-MgO / Fe + (Fe_xO)_{slag} + Ag / Fe, \dots \dots \dots \dots (cell \; 3)$$
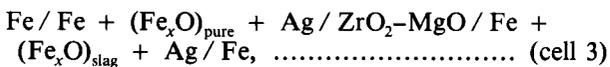
which corresponds to the cell reaction

$$(Fe_xO)_{pure} = (Fe_xO)_{slag}. \dots \dots \dots \dots (4)$$

If the operation of the cell is assumed to be reversible, and if pure liquid Fe_xO in equilibrium with iron is taken as the standard state of iron oxide, the following equation can be derived for the calculation of Fe_xO activity:

$$\ln a(Fe_xO) = \frac{-2F}{RT} [E(2) - E(1)], \dots \dots \dots (5)$$

where $E(1)$ and $E(2)$ are the measured open-circuit emf's of cells 1 and 2 respectively, F is the Faraday constant, R the gas constant, and T the absolute temperature.

It should be noted that errors in the measured emf may arise from electronic conduction in the solid electrolyte at low oxygen potentials and high temperatures[6]. However, from a detailed investigation of the electronic conduction in commercial zirconia electrolytes[4,6] and measurements by the present authors[7], it is concluded that the electronic conduction in the electrolytes used is negligibly under the experimental conditions pertaining to this study ($T = 1673$ K and $PO_2 \geq 1,65 \cdot 10^{-11}$ atm.).

Experimental

Apparatus

The experimental apparatus, shown in Fig. 1, consists basically of a purification train for argon and an alumina reaction tube (65 mm in internal diameter, 75 mm in external diameter, and 750 mm in height) contained inside a silicon carbide resistance furnace. The reaction tube and crucible assembly are shown in Fig. 2. An alumina guide tube (12 mm in internal diameter, 15 mm in external diameter, and 700 mm in height) is incorporated in the reaction-tube assembly. The upper end of the reaction tube is sealed by a water-cooled brass fitting with rubber O-rings. All inserts through the brass fitting are likewise sealed by means of rubber O-rings.

The arrangement of the electrochemical cell, which can be expressed as

$$Mo / Mo + MoO_2 / ZrO_2-MgO / Fe + (Fe_xO)_{slag} + Ag / Fe, \dots \dots \dots \dots (cell \; 2)$$
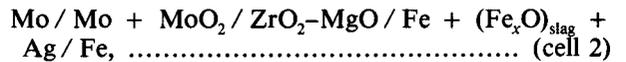
consists of a ZrO_2–9 mol per cent MgO solid electrolyte, an $(Mo + MoO_2)$ reference electrode, and an $(Fe + FeO_{slag})$ electrode. The isostatically pressed and sintered zirconia tubes (4 mm in internal diameter, 6 mm in outside diameter, and 50 mm in height) were supplied by Nippon Kagaku Togyo Co. Fig. 3 illustrates the construction of the ZrO_2 probe. Since MoO_2 is not commercially available, a mixture of Mo and MoO_3 was used as the initial reference powder, the MoO_2 being prepared *in situ*, via the reaction

$$2 MoO_3 + Mo = 3 MoO_2. \dots \dots \dots \dots (6)$$
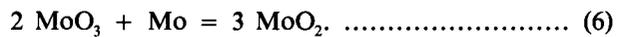
A molybdenum rod (3,12 mm in diameter and 800 mm in length) was placed inside the zirconia tube, which was subsequently filled with a mixture of Mo and MoO_3 containing 75 per cent Mo (by mass). The mixture was prepared by the dry mixing of analytical-grade Mo and MoO_3 powders. The molybdenum rod, which served as an electrical lead to the reference electrode, was cemented onto the zirconia tube by means of alumina cement. The electrical circuit of the cell was completed by liquid silver and an iron rod welded to the iron crucible (25 mm in internal diameter, 35 mm in external diameter, and 90 mm in height). To correct for the thermal emf of the dissimilar electrical leads, the thermal emf of the iron–molybdenum couple was determined in a separate experiment.

Procedure

The alumina protection crucible, inlet tubes, thermocouple sheath, and iron crucible containing approximately 15 g of slag and 25 g of high-purity silver were positioned inside the reaction tube as shown in Fig. 2. Synthetic slags were prepared from analytical-grade CaO, SiO_2, and Fe_2O_3 powders. Complex slags were prepared from an industrial slag used for the external desiliconization of hot metal[8]. After the furnace had been sealed and evacuated to ensure gas tightness, purified argon gas was introduced into the reaction tube. The purification of argon was done by the passing of spectrographic argon successively through silica gel, magnesium perchlorate, phosphorus pentoxide, and copper turnings, held at 873 K (Fig. 1). The furnace was then heated to 773 K, re-evacuated to ensure dehydration, and subsequently heated to 1673 K in a stream of purified argon. At that temperature, the oxygen probe was positioned inside the guide tube and slowly moved downwards until the lower end of the probe was just above the slag melt. After an equilibration time of approximately 20 minutes, the probe was slowly immersed in the melt so that it contacted the slag as well as the silver without touching the bottom of the crucible. As soon as a stable emf was obtained, the probe was raised to a position just above the slag melt. This procedure was repeated until the reproducibility of the emf's was confirmed. The probe was subsequently removed from the guide tube, and a sample of slag was
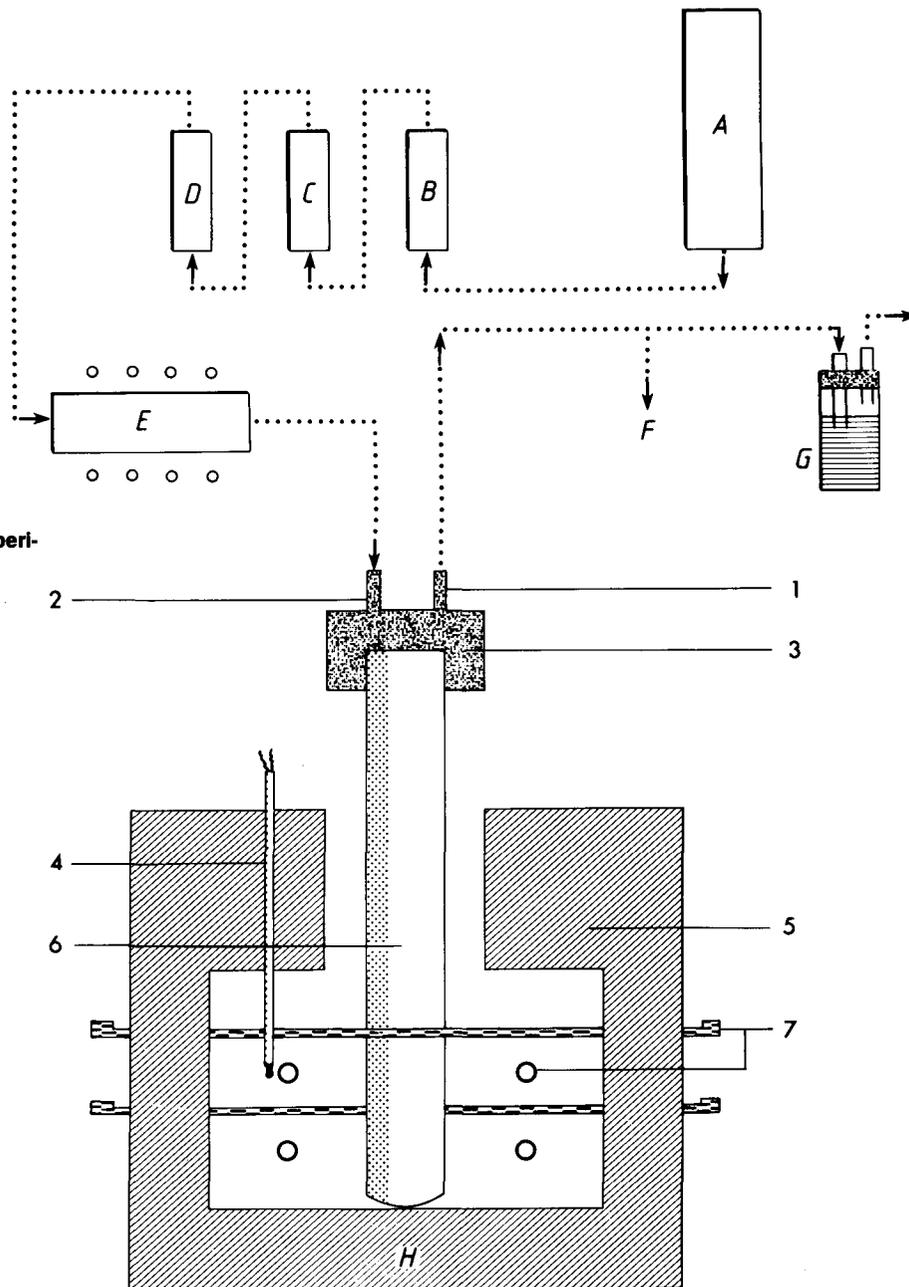
Fig. 1—Schematic diagram of the experimental apparatus

A Spectrographic argon
B Silica gel
C Magnesium perchlorate
D Phosphorus pentoxide
E Copper turnings at 873 K
F Vacuum pump
G Air trap

1 Argon outlet
2 Argon inlet
3 Water-cooled brass fitting
4 Furnace thermocouple
5 Furnace
6 Reaction tube
7 Silicon carbide

taken by the dipping of a steel rod into the slag. The sample was quenched in water and analysed for ferrous iron, total iron, silver, and other oxides by wet-chemical analysis and atomic-absorption spectrography. In order to change the slag composition, small pellets of iron oxide or mixed oxide powders were added to the melt. The slag was stirred with an iron rod to accelerate the attainment of equilibrium. Approximately one hour was allowed for the attainment of equilibrium. Whenever the reaction tube was opened, the tube was re-evacuated and flushed with argon. A new oxygen probe was used whenever the slag composition was changed. Normally, slags of 4 to 6 different compositions were studied during an experimental run.

A Pt6Rh–Pt30Rh thermocouple, placed alongside the alumina protection crucible, was used to measure the temperature. The measurements indicated that the tem-

perature gradient over the length of the crucible was less than 2 K, and, that the overall error was less than 3 K. All the measurements were conducted at 1673 $\pm$3 K. An electrometer with a 10^{14} Ω input impedance and an accuracy of 0,01 mV was used for the emf measurements. The electrometer was coupled to a chart recorders, allowing the emf to be recorded continuously.

To evaluate the validity of the *in situ* preparation of MoO_2, and to verify that reaction 6 went to completion, the phases present in the reference electrode after the emf measurements had been taken were examined by X-ray diffraction. Since only Mo and MoO_2 were detected, it is concluded that the slow heating of the probe, together with the equilibration time before immersion into the slag, resulted in attainment of the equilibrium oxygen potential of the (Mo + MoO_2) mixture before the actual emf measurements were made.
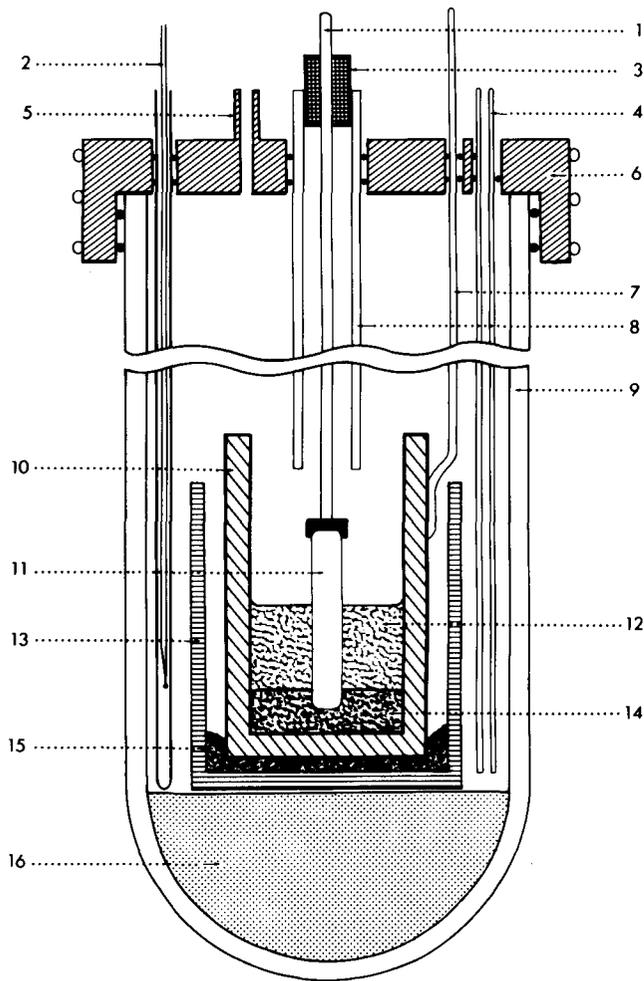
Fig. 2—Reaction tube and crucible assembly used for the direct measurement of iron oxide activity in liquid slags

1	Molybdenum rod	9	Alumina reaction tube
2	Pt6Rh–Pt30Rh thermo-	10	Iron crucible
	couple	11	Zirconia oxygen probe
3	Rubber stopper	12	Liquid slag
4	Alumina argon inlet	13	Alumina protection cru-
5	Argon outlet		cible
6	Water-cooled brass	14	Liquid silver
	fitting	15	Chromium oxide powder
7	Iron rod	16	Alumina powder
8	Alumina guide tube		

Fig. 3—Construction of the zirconia oxygen probe

Influence of Slag Attack

In the past, the dissolution of solid electrolytes in iron oxide slags impeded the direct measurement of iron oxide activities. However, it was shown recently that the rate of dissolution of magnesia-stabilized zirconia is slow enough for stable emf readings to be obtained for short periods of time[4]. It should be emphasized, however, that slag penetration can occur to a significant extent even if the rate of dissolution is slow. This is especially true when the solid electrolyte contains a second-phase precipitate on the grain boundaries, which can react with iron oxide slags[9]. Slag that penetrates the solid electrolyte in this way will induce a certain amount of electronic conduction in the electrolyte, resulting in an erroneous open-circuit emf measurement. It was accordingly considered necessary to evaluate the extent of slag penetration in the electrolyte so that the influence of such slag penetration on the measured cell poten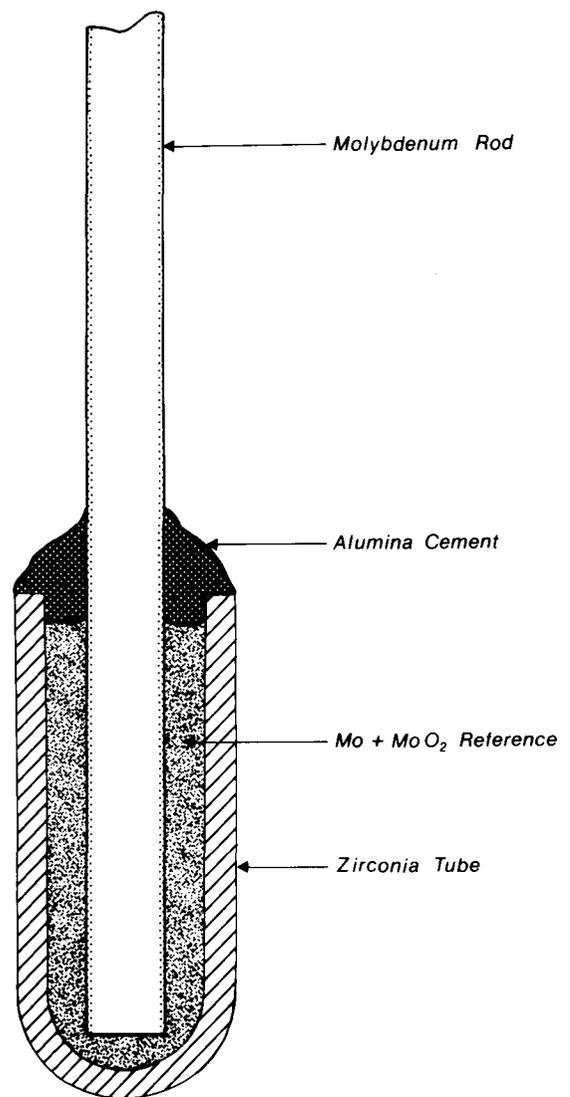tial could be assessed. This was done by an examination of the cross-sections of the electrolyte used in the oxygen probe by means of scanning electron microscopy and microprobe X-ray analysis.

A typical emf response recorded during emf measurements in pure iron oxide is shown in Fig. 4. The reversibility of the cell was checked by short-circuiting of the cell for approximately 2 seconds. When the short-circuit was removed, the cell potential returned to the equilibrium value within 10 seconds, as shown in Fig. 4. Stable emf readings were obtained for approximately 4 minutes after the probe had been immersed in the iron oxide melt. After about 4 minutes, the emf of the cell decreased abruptly, as shown in Fig. 4. This sudden decrease in emf is attributed to the combined effect of the dissolution of the zirconia electrolyte in the reactive iron oxide slag and slag penetration into the electrolyte. This conclusion was confirmed by the observation that the wall thickness of
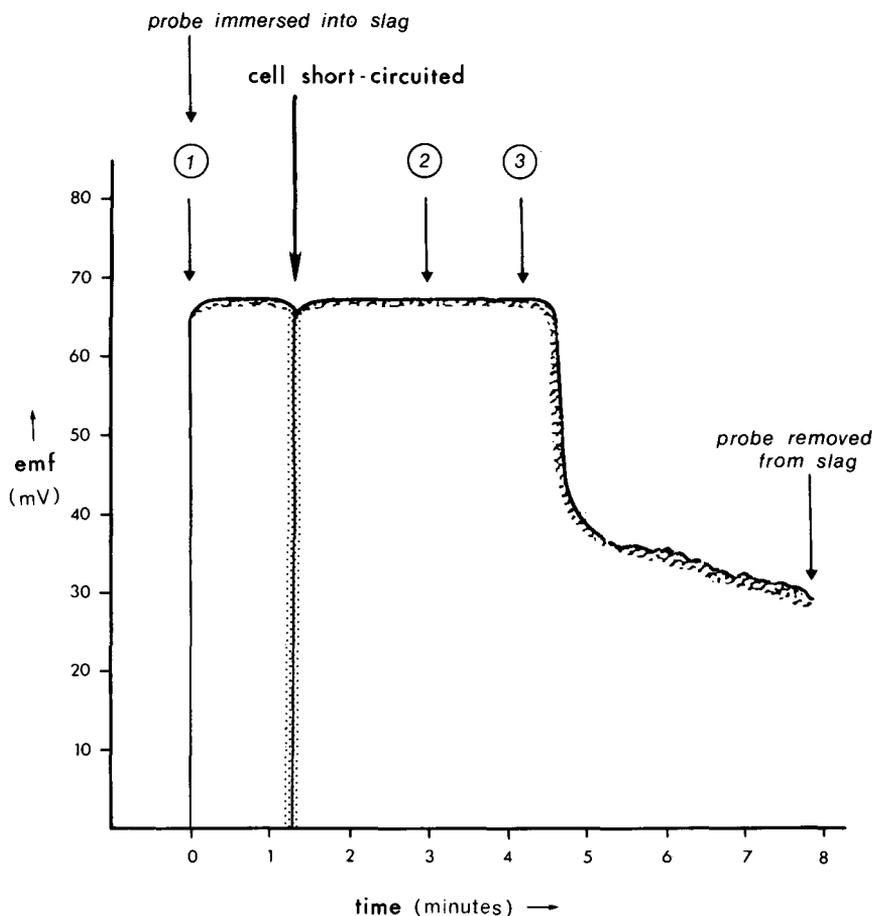
Fig. 4—Typical emf values recorded during measurements in pure liquid iron oxide at 1673 K

the tube decreased with time, and that there was extensive slag penetration into the zirconia tube at about that time, as shown in Fig. 5.

It should be noted that the slag attack was most serious in pure liquid iron oxide. The durability of the solid electrolyte depends mainly on the iron oxide content of the slag and increases significantly with a decrease in that content.

From the cell response in the most corrosive medium—pure iron oxide—as shown in Fig. 4, it is evident that a stable emf reading is obtained for at least 4 minutes after the probe has been immersed in the slag. During normal cell operation, however, stable emf readings were obtained within 10 to 20 seconds of the immersion, and the total immersion time seldom exceeded 30 seconds. Slag attack of the zirconia was consequently minimized and did not affect the measured cell potentials under normal operating conditions.

Results and Discussion
Standard Free Energy of Formation of Liquid Iron Oxide

As a check on the reliability of the oxygen probe in direct contact with liquid slags, cell 1 was used in a determination of the standard free energy of formation of liquid Fe_xO, given by the equation

$$\Delta G^\circ(Fe_xO) = \frac{1}{2} \, RT \ln P_{O_2}[Fe + (Fe_xO)_{pure}], \quad \ldots \quad (7)$$

where $P_{O_2}[Fe + (Fe_xO)]_{pure}$ is the oxygen partial pressure of pure liquid Fe_xO in equilibrium with δ iron.

The open-circuit emf of cell 1 is given by

$$E(1) = E(T) - \frac{RT}{4F} \ln \left\{ \frac{P_{O_2}[Fe + (Fe_xO)_{pure}]}{P_{O_2}[Mo + MoO_2]} \right\}, \quad (8)$$

where $P_{O_2}[Fe + (Fe_xO)_{pure}]$ and $P_{O_2}[Mo + MoO_2]$ are the equilibrium oxygen partial pressures of pure liquid Fe_xO in equilibrium with δ iron and the $(Mo + MoO_2)$ reference mixture respectively. $E(T)$ is the thermal emf between Fe and Mo, which was measured as $23,0 \pm 1,0$ mV at 1673 K. According to Iwase *et al.*[10], the oxygen potential of the $(Mo + MoO_2)$ reference electrode is given by

$$RT \ln P_{O_2}[Mo + MoO_2] = -576100 + 169,2 \, T$$
$$\text{J/mol of } O_2. \quad \ldots\ldots\ldots\ldots\ldots\ldots\ldots\ldots\ldots\ldots\ldots\ldots\ldots\ldots\ldots\ldots \quad (9)$$

The standard free energy of formation of liquid Fe_xO was calculated by the substitution into equation (7) of the value of $P_{O_2}[Fe + (Fe_xO)_{pure}]$ obtained from equation (8).

Table I shows a comparison between the values of $\Delta G^\circ(Fe_xO)$ obtained in this way and data reported in the literature. It is evident that there is good agreement between the present work and the values reported by earlier investigators. The conclusion can rightfully be made that the technique used in this investigation is reliable, and that the open-circuit emf values so obtained can be used in the calculation of the activity of iron oxide.

Activities of Iron Oxide in Fe_xO-M_xO_y Slags

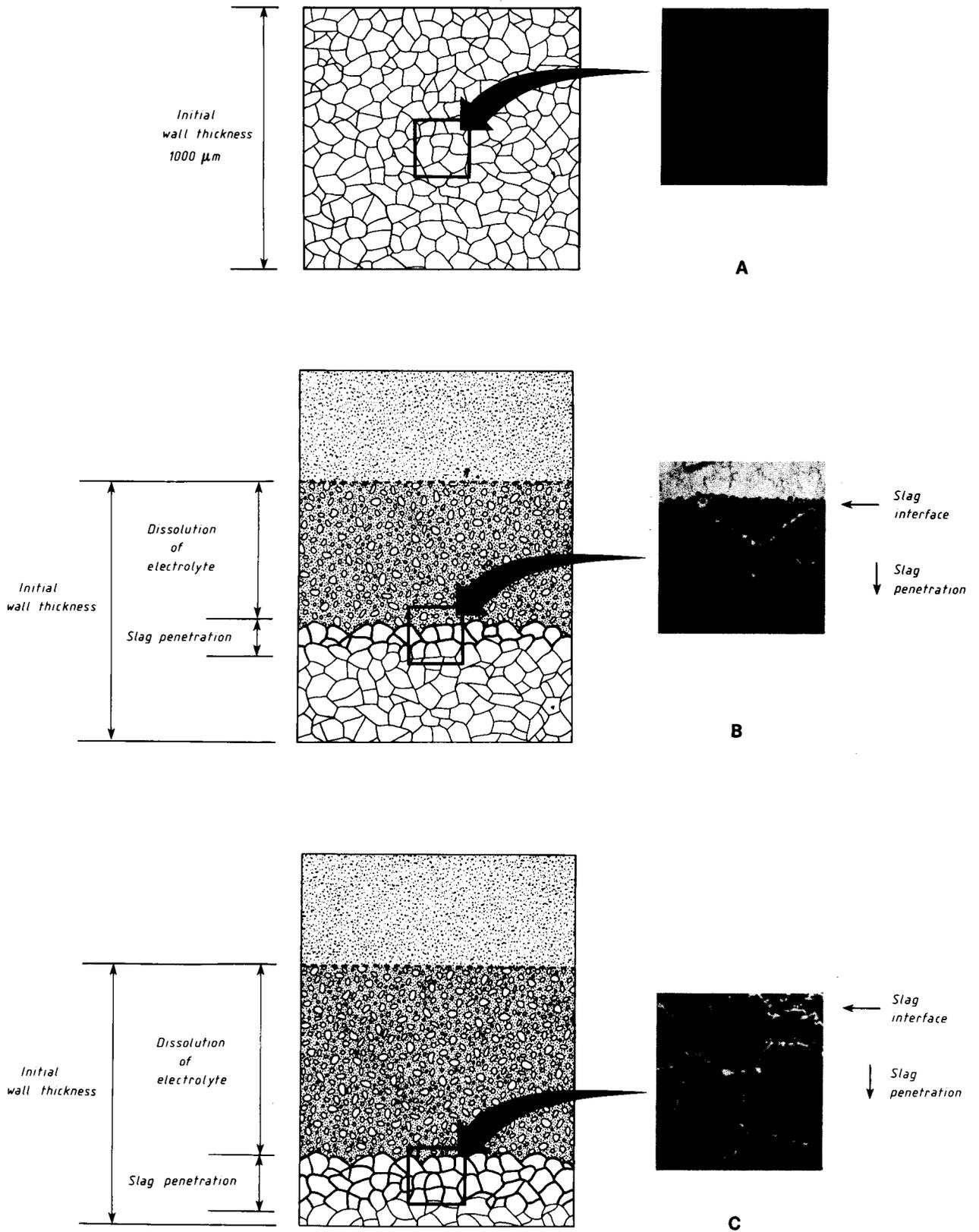In an investigation of the performance of the oxygen

Fig. 5—Schematic illustration of electrolyte dissolution and slag penetration into magnesia-stabilized zirconia after different immersion times, as observed by scanning electron microscopy, together with characteristic X-ray images of Fe on cross-sections of the electrolyte tubes

A Before immersion in the slag   B After an immersion time of approximately 3 minutes
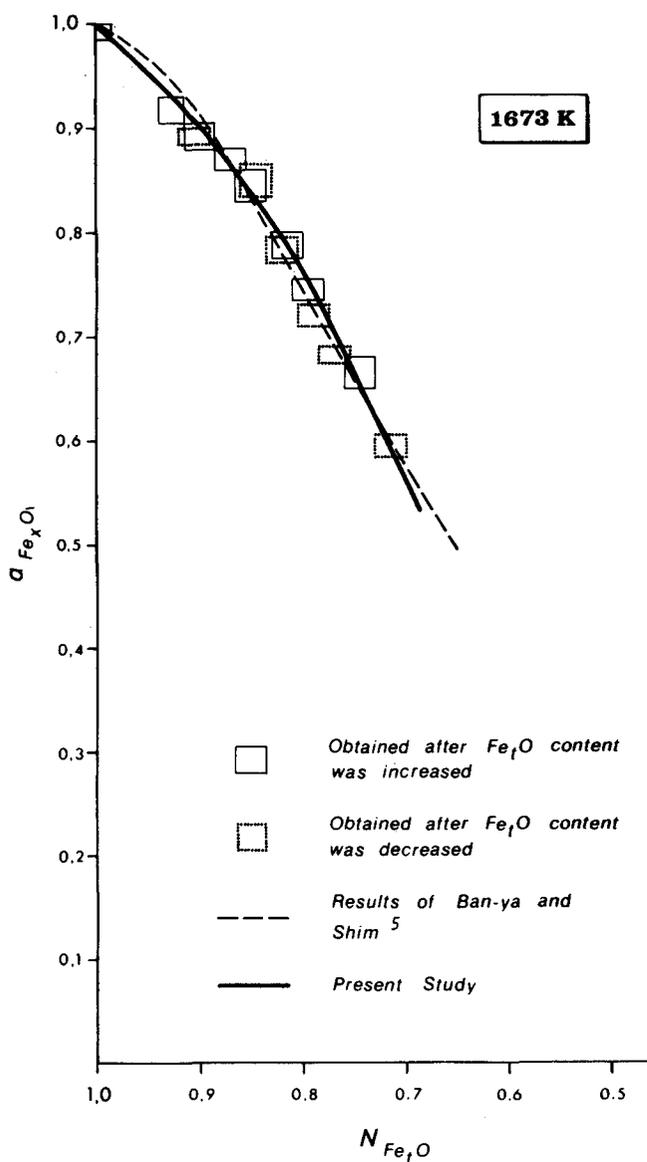
C After an immersion time of approximately 4 minutes

Fig. 6—The activity of Fe$_x$O as a function of iron content in an Fe$_x$O–CaO slag at 1673 K

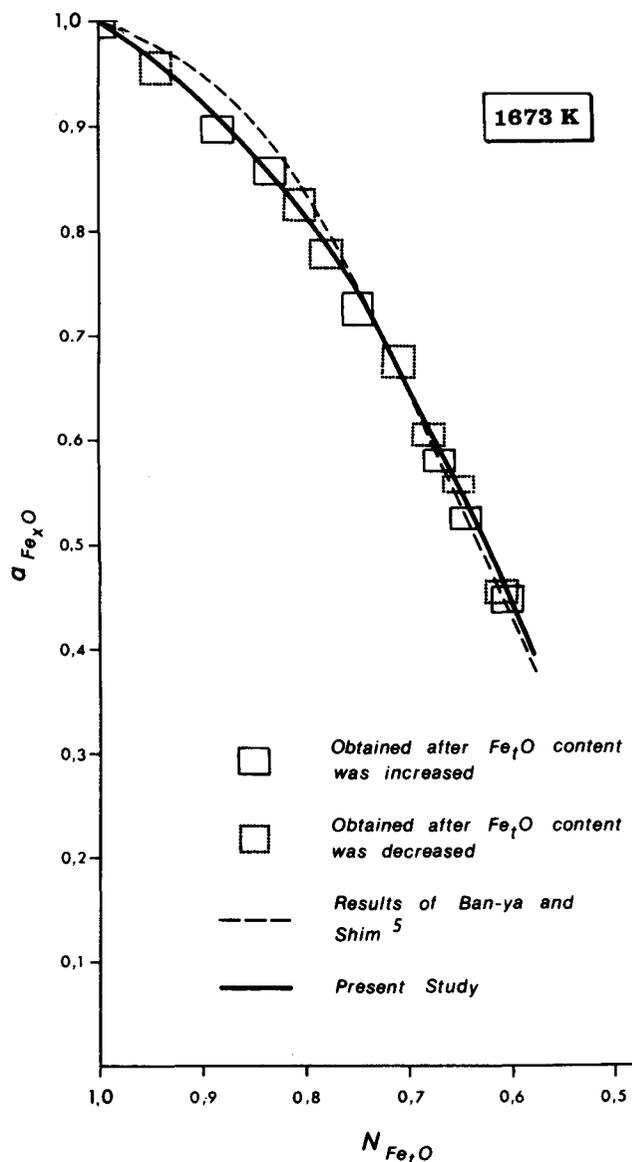**Fig. 7—The activity of Fe$_x$O as a function of iron content in an Fe$_x$O–SiO$_2$ slag at 1673 K**

TABLE I

STANDARD FREE ENERGY OF FORMATION OF LIQUID
IRON OXIDE AT 1673 K

Experimental technique	$\Delta G°(Fe_xO)$ kJ/mol	Reference
(CO + CO$_2$) equilibrium	− 156,0	Darken and Gurry[11]
Compilation	− 156,3	Elliot and Gleiser[12]
Electrochemical	− 154,6 ± 0,6	Iwase et al.[4]
Electrochemical	− 154,9 ± 0,9	Present study

probe in basic, as well as acidic, slags, Fe$_x$O activities were measured in synthetic Fe$_x$O–CaO and Fe$_x$O–SiO$_2$ slag. The activities of Fe$_x$O relative to a standard state of pure liquid iron oxide in equilibrium with δ iron at 1673 K were obtained from the experimental values of E(1) and E(2) in equation (5), and are shown in Figs. 6 and 7 for the Fe$_x$O–CaO and Fe$_x$O–SiO$_2$ systems respectively. The slag composition is expressed as Fe$_t$O, which

denotes the total iron content expressed as stoichiometric FeO.

To confirm the attainment of equilibrium during the experimental runs, the equilibrium at each Fe$_t$O content was approached from both a higher and a lower Fe$_t$O content. The good reproducibility of the Fe$_x$O activity obtained in this manner, as shown in Figs. 6 and 7, confirms that equilibrium was attained during the experimen-

tal runs. The total uncertainty of the experimental data, i.e. uncertainty resulting from errors in the measurements of slag composition, temperature, and the standard deviation of the emf measurements, are indicated by the areas of the quadrangles. The uncertainty of the activity data was calculated from the equation

$$\frac{d[a(Fe_xO)]}{a(Fe_xO)} = d[\ln a(Fe_xO)] \le$$

$$\left| \frac{2F}{RT} \right| \left| dE(1) \right| + \left| \frac{2F}{RT} \right| \left| dE(2) \right| + \left| \frac{2FE(1)}{RT^2} \right| \left| dT \right| +$$

$$\left| \frac{1FE(2)}{RT^2} \right| \left| dT \right| \quad \dots\dots\dots\dots\dots\dots\dots\dots\dots\dots\dots \text{(10)}$$

(where ‖ denotes the absolute value), which is based on the differential of equation (5). The uncertainty in the slag composition did not exceed 0,015 mol fraction, and arose from the slight dissolution of zirconia in the melt and from errors in the chemical analysis. The experimental results and uncertainty of the individual measurements are summarized in Tables II and III.

TABLE II
EXPERIMENTAL RESULTS FOR THE Fe_xO-CaO SYSTEM AT 1673 K

Melt no.	emf mV	$N(Fe_tO)$	$a(Fe_xO)$
1.1	66,7 ± 0,5	1,000 ± 0,015	1,000 ± 0,017
2.1	84,0 ± 0,5	0,816 ± 0,015	0,787 ± 0,014
2.2	88,0 ± 0,2	0,793 ± 0,015	0,744 ± 0,010
3.1	96,0 ± 0,8	0,743 ± 0,015	0,666 ± 0,015
4.1	103,9 ± 0,4	0,713 ± 0,015	0,597 ± 0,010
4.2	94,1 ± 0,1	0,771 ± 0,015	0,684 ± 0,008
4.3	90,2 ± 0,4	0,792 ± 0,015	0,722 ± 0,012
4.4	84,4 ± 0,2	0,820 ± 0,015	0,782 ± 0,011
5.1	66,7 ± 0,5	1,000 ± 0,015	1,000 ± 0,017
5.2	78,8 ± 0,6	0,853 ± 0,015	0,845 ± 0,016
6.1	78,6 ± 0,4	0,855 ± 0,015	0,848 ± 0,014
6.2	76,7 ± 0,2	0,872 ± 0,015	0,870 ± 0,012
6.3	75,0 ± 0,3	0,902 ± 0,015	0,891 ± 0,013
6.4	72,9 ± 0,3	0,923 ± 0,015	0,918 ± 0,013
6.5	75,2 ± 0,1	0,902 ± 0,015	0,889 ± 0,011

TABLE III
EXPERIMENTAL RESULTS FOR THE Fe_xO-SiO$_2$ SYSTEM AT 1673 K

Melt no.	emf mV	$N(Fe_tO)$	$a(Fe_xO)$
1.1	95,0 ± 0,6	0,712 ± 0,015	0,675 ± 0,013
1.2	103,0 ± 0,4	0,679 ± 0,015	0,604 ± 0,010
1.3	108,7 ± 0,2	0,651 ± 0,015	0,558 ± 0,008
1.4	123,4 ± 1,0	0,608 ± 0,015	0,455 ± 0,012
4.1	66,8 ± 0,5	1,000 ± 0,015	1,000 ± 0,017
4.2	80,5 ± 0,5	0,805 ± 0,015	0,826 ± 0,014
4.3	74,5 ± 0,4	0,885 ± 0,015	0,897 ± 0,014
5.1	123,2 ± 0,6	0,610 ± 0,015	0,456 ± 0,009
5.2	113,1 ± 0,6	0,643 ± 0,015	0,525 ± 0,010
5.3	105,9 ± 0,5	0,668 ± 0,015	0,580 ± 0,011
5.4	89,8 ± 0,4	0,752 ± 0,015	0,726 ± 0,012
6.1	78,0 ± 0,5	0,944 ± 0,015	0,955 ± 0,017
6.2	85,0 ± 0,4	0,782 ± 0,015	0,776 ± 0,013

In analyses of the accuracy of the Fe_xO activities determined in this study, it is informative to compare the present results with those measured by a different experimental technique. The activities of iron oxide measured in the present investigation are compared with the values obtained by Ban-ya and Shim[5] in a similar slag, using the conventional gas-equilibrium technique. Although these authors did not analyse the uncertainties of their experimentally determined activities, it appears that the present results are in good agreement with their measurements. Thus, on the basis of these results, it is reasonable to place a good measure of confidence in the ability of the present experimental technique to accurately measure Fe_xO activities in a variety of slag systems.

Activities of Iron Oxide in Complex Slags

The experimental technique described above was extended to the measurement of Fe_xO activities in the complex slags used for the external desiliconization of hot metal[8]. In such a process, iron oxide powder is injected into the hot-metal product of the blast furnace, resulting in the oxidation of silicon in the melt. The reaction of silicon with iron oxide can be expressed as

$$2 \, (Fe_xO)_{slag} + (Si)_{Fe} = (SiO_2)_{slag} + 2x \, (Fe). \quad \dots \text{(11)}$$

As the reaction proceeds, the iron oxide is reduced and the silicon, manganese, and titanium in the hot metal are oxidized simultaneously. The complex slags used in this study were prepared from samples of slag taken during the final stages of external desiliconization of hot metal[8] and are summarized in Table IV. Fig. 8 shows the measured activities relative to a standard state of pure liquid Fe_xO in equilibrium with δ iron at 1673 K. The standard deviation of the individual measurements and the accuracy of the activity data calculated from equation (10) are also summarized in Table IV.

Owing to a paucity of data on the activity of iron oxide in complex slags at iron-making temperatures[13], the Fe_xO activities shown in Fig. 8 were compared with the results of Turkdogan and Pearson[14], which were obtained at steel-making temperatures. According to those authors, the Fe_xO activity in complex slags is independent of temperature, and the influence of slag composition on the activity can be approximated from a consideration of the pseudoternary system (CaO + MgO + MnO)-Fe_xO-(SiO$_2$ + P$_2$O$_5$). In Fig. 9, the Fe_xO activities obtained from the smoothed curve in Fig. 8 are compared with the results of Turkdogan and Pearson. As shown in Fig. 9, the activities reported by those authors at temperatures between 1823 and 1923 K differ significantly from those obtained in the present study at 1673 K, especially at low Fe_tO concentrations.

From these results it seems that the available activity data of Turkdogan and Pearson, which are applicable to typical steel-making slags, cannot be used in the calculation of Fe_xO activities in the slag systems typically used in external hot-metal treatment. This conclusion is in agreement with the results of Iwase *et al.*[2], who showed that the data of Turkdogan and Pearson are also not applicable to the slag systems used in the external dephosphorization of hot metal. Owing to the limited data available, the reason for this apparent anomaly is not fully understood at this stage but is the subject of further investigation.

TABLE IV
EXPERIMENTAL RESULTS FOR THE COMPLEX SLAGS AT 1673 K

Melt no.	emf mV	$a(Fe_xO)$	Chemical composition (mol %)										
			Fe_xO	SiO_2	Al_2O_3	CaO	MgO	MnO	K_2O	Na_2O	TiO_2	P_2O_5	CaS
1.1	158,6 ± 0,4	0,279 ± 0,005	35,4	44,5	2,5	1,0	1,3	13,9	0,1	0,2	1,2	0,1	0,5
1.2	106,5 ± 0,5	0,575 ± 0,010	55,0	31,1	1,7	0,7	0,9	9,7	0,1	0,1	0,8	0,0	0,3
1.3	97,6 ± 1,0	0,651 ± 0,015	61,3	27,0	1,5	0,6	0,8	8,4	0,1	0,1	0,7	0,0	0,3
1.4	82,3 ± 0,3	0,805 ± 0,012	73,7	18,2	1,0	0,4	0,5	5,6	0,1	0,1	0,5	0,0	0,1
1.5	77,5 ± 0,5	0,860 ± 0,015	78,8	14,5	0,8	0,3	0,4	4,5	0,1	0,1	0,4	0,0	0,1
2.1	157,3 ± 0,8	0,284 ± 0,007	35,4	44,5	2,5	1,0	1,3	13,9	0,1	0,2	1,2	0,1	0,5
2.2	130,8 ± 0,6	0,411 ± 0,008	43,4	39,0	2,2	0,9	1,1	12,1	0,1	0,2	1,0	0,1	0,4
2.3	124,9 ± 1,0	0,446 ± 0,011	47,6	36,0	2,1	0,8	1,0	11,2	0,1	0,2	1,0	0,1	0,3
2.4	95,4 ± 0,2	0,671 ± 0,009	61,8	26,3	1,5	0,6	0,7	8,2	0,1	0,1	0,7	0,0	0,3
3.1	66,7 ± 0,5	1,000 ± 0,017	100,0	0,0	0,0	0,0	0,0	0,0	0,0	0,0	0,0	0,0	0,0
3.2	68,8 ± 0,3	0,971 ± 0,014	94,9	2,8	0,2	0,0	0,1	0,8	0,0	0,0	0,1	0,0	0,0
3.3	69,2 ± 0,3	0,965 ± 0,014	94,7	2,8	0,2	0,0	0,1	0,8	0,0	0,0	0,1	0,0	0,0
3.4	71,3 ± 0,2	0,938 ± 0,012	90,2	6,3	0,4	0,2	0,2	2,0	0,0	0,0	0,2	0,0	0,1
3.5	74,5 ± 0,2	0,897 ± 0,012	83,0	11,4	0,7	0,2	0,3	3,6	0,0	0,1	0,3	0,0	0,1
3.6	88,2 ± 0,5	0,740 ± 0,013	67,5	22,5	1,3	0,5	0,6	7,1	0,1	0,1	0,6	0,0	0,1
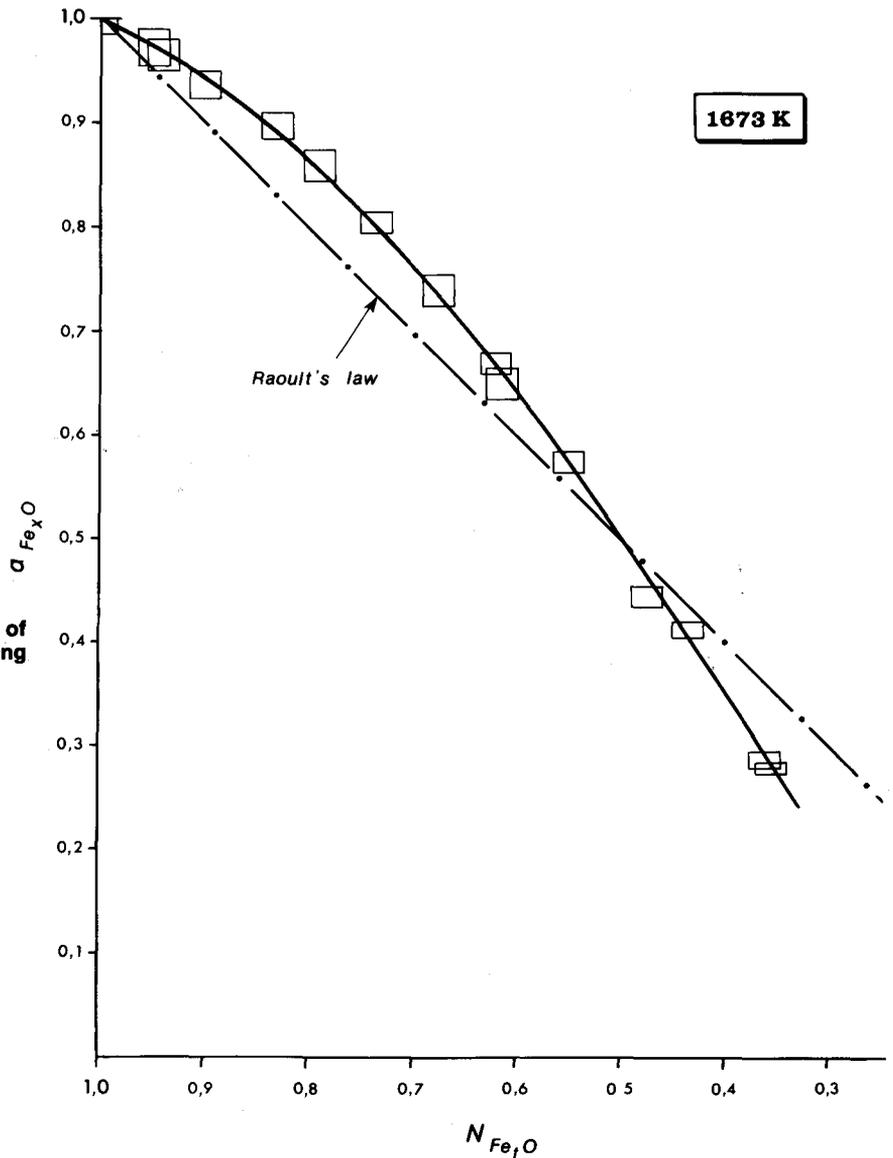
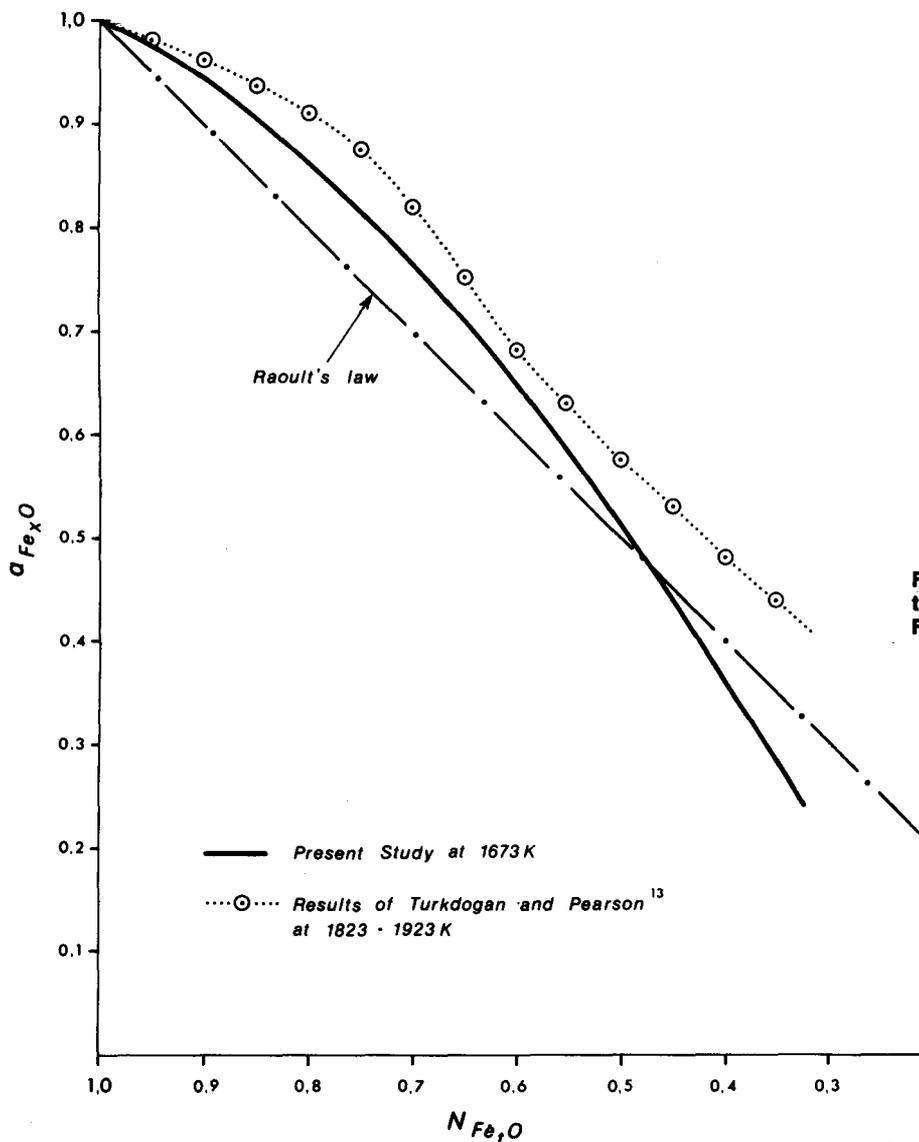Fig. 8—The activity of Fe_xO as a function of iron content in complex Fe_xO-containing slags at 1673 K

1673 K

Raoult's law

Fig. 9—A comparison between the Fe_xO activities obtained from the smoothed curve in Fig. 8 and those of Turkdogan and Pearson[14]

—— Present Study at 1673 K

····⊙···· Results of Turkdogan and Pearson[13] at 1823 · 1923 K

Conclusions

(1) The good agreement of the experimental results obtained in this study with the work of earlier investigators proves that the electrochemical technique used can be successfully applied to the measurement of iron oxide activities in a variety of slag systems at iron-making temperatures.

(2) From the results obtained in the present study, as well as from the results of other recent investigations, it seems that the data in the literature on the activity of iron oxide in steel-making slags at steel-making temperatures cannot be extrapolated to cover the external refining of blast-furnace hot metal at iron-making temperatures.

(3) It is recommended that the experimental technique described in this paper should be used in the measurement of iron oxide activity in the slag systems used in the new external refining processes for hot metal, which may be introduced into the South African steel industry.

Acknowledgements

References

1. BAN-YA, S. HINO, M., and TAKEZOE, H. *Second International Symposium on Metallurgical Slags and Fluxes.* Nevada, Nov. 1984, p. 395.
2. IWASE, M., YAMADA, N., AKIZUKI, H., and ICHISE, E. *Arch. Eisenhüttenwes.,* vol. 55, no. 10. 1984. p. 471.
3. IWASE, M., ICHISE, E., YAMADA, N., and NISHIDA, K. *ISS Trans.,* vol. 4. 1984. p. 47.
4. IWASE, M., YAMADA, N., NISHIDA, K., ICHISE, E. *ISS Trans.,* vol. 4. 1984. p. 69.
5. BAN-YA, S., and SHIM, J-D. *Can. Metall. Q.,* vol. 21, no. 4. 1982. p. 319.
6. IWASE, M., ICHISE, E., TAKEUCHI, M., and YAMASAKI, T. *Trans. Japan. Inst. Metals,* vol. 25, no. 1. 1984. p. 43.
7. VAN WIJNGAARDEN, M.J.U.T. University of Pretoria, Ph.D. Thesis, To be published.

8. PIENAAR, I.C. University of Pretoria, M.Eng. Dissertation. To be published.
9. KAWAKAMI, M., GOTO, K.S., and MATSUOKA, M. *Metall. Trans.*, vol. 11B. Sep. 1980. p. 463.
10. IWASE, M., YASUDA, M-O., and MORI, T. *Electrochimica Acta*, vol. 24. 1979. p. 261.
11. DARKEN, L.S., and GURRY, R.W. *J. Amer. Chem. Soc.*, vol. 68. 1946. p. 798.
12. ELLIOTT, J.F., and GLEISER, M. *Thermochemistry for steelmaking*. Addison-Wesley, 1960. vol. 1. p. 179.
13. VEREIN DEUTSCHER EISENHÜTTENLEUTE (ed.). *Slag atlas*. Verlag Stahleisen M.B.H., 1981.
14. TURKDOGAN, E.T., and PEARSON, J. *J. Iron Steel Inst.*, vol. 173. 1953. p. 217.

Multi-phase flow

BHRA, The Fluid Engineering Centre, will hold its Third International Conference on Multi-phase Flow at The Hague Congress Centre, from 18th to 20th May, 1987.

Multi-phase flows are designed into many engineering applications, particularly in the petroleum, process, and power-generation industries. The understanding of these flows has become central to the development of improved systems, for example, in the petroleum industry, where an understanding of complex multi-phase flows is essential to the economic design and operation of oil and gas recovery and transportation. Pressure drop, holdup, flow regime, and transient phenomena must all be taken into account when designing, sizing, and specifying well-bores, flowlines, gas–liquid and liquid–liquid separation equipment. In addition, fluid property effects and phase behaviour are strongly influenced by the operating temperature and pressure of the system; in particular, the formation of emulsions and hydrates can give rise to problems in pipeline and separation equiment. As offshore pipelines run into greater depths and as more marginal fields are exploited, oversizing becomes less acceptable. Reliable multi-phase design information on oil–water–gas–sand flows is urgently required to promote the development of this new technology and to optimize pipeline systems, slugcatchers, and separation equipment.

It is hoped that the scope of the Conference will promote the interchange between heat-transfer orientated and petroleum orientated multi-phase research.

Designers, operators, and researchers will be able to discuss current practice and theory, as well as the future needs of industry, at this meeting.

The Conference will deal with physical modelling, mathematical modelling, and practical experience of gas–liquid, liquid–liquid, and gas–liquid–solid flows in pipelines and equipment, with particular emphasis on oil and gas production and transportation systems. Relevant papers from non-petroleum systems and those dealing with instrumentation and small amounts of solids will also be considered.

Subject areas of particular interest are

● Operational experience of multi-phase pipelines and equipment
● Multi-phase flow prediction, effects of scale, and comparisons with site data
● Advances in equipment for total sub-sea production and transportation
● Practical measurement, instrumentation, and control for multi-phase flows, including flow–pattern detection
● Model and prototype studies of flows in oil–gas pipelines and equipment

● Computer-aided design of multi-phase systems with comparison against existing data
● Behaviour of multi-phase pipelines and equipment under transient conditions caused by topography, feed variations, plant upset, failure, or loss of containment
● Experience with floating production systems, with particular emphasis on the flows of flexible risers and the performance of separation and processing equipment in the dynamic environment
● Flows through components such as safety valves, chokes, bends, and tees
● Separation of gas–liquids and liquid–liquids in oil and gas systems
● Erosion–corrosion in multi-phase systems.

Authors are invited to submit titles and synopses of papers appropriate to the subject and scope of this Conference to reach BHRA as soon as possible but not later than 1st May, 1986. Completed manuscripts having a text of approximately 4000 words will be required by 6th October, 1986.

Authors should please note that

– In all cases work should be original and not have been published or offered for publication elsewhere.
– Papers must be submitted and presented in English.
– Papers accepted for presentation will be published by BHRA in a bound volume and, where possible, issued to delegates before the meeting. The volume will be made available for general sale at a later date.
– Authors of accepted papers are expected to present their papers and to attend the meeting as delegates, but will be entitled to a substantial reduction in the Conference fees.

An exhibition is planned to enable participating organizations to display company literature and associated material throughout the Conference. Additionally, a full page black-and-white advertisement may be placed in the Volume of Papers, which is circulated worldwide. The A4 camera-ready copy of the advertisement should reach BHRA at the address below no later than 6th February, 1987.

Further details are available from

Conference Organizer
3rd Multi-phase Flow
BHRA, The Fluid Engineering Centre
Cranfield
Bedford MK43 OAJ
England.
Telephone: 0234 750422. Telex: 825059 BHRA G.